

# Swirl effects on variable-density jet mixing in confined flows

Ramin Majidi and Ronald M. C. So

Mechanical and Aerospace Engineering Department,  
Arizona State University, Tempe, AZ 85287, USA

Received March 1987 and accepted for publication July 1987

An experimental investigation on swirl effects on inhomogeneous confined jet mixing in a combustor configuration is reported. The confined swirling flow was simulated by a swirler with a central jet mounted in a cylindrical tube. Helium and air jets set at different velocities were injected into the confined swirling air flow. The resulting flow fields due to two vane swirlers with constant vane angles of  $35^\circ$  and  $66^\circ$  were compared. Results show that the  $35^\circ$  vane swirler produces a solid-body rotation core with a slope about twice that created by the  $66^\circ$  vane swirler. It is the behavior of this solid-body rotation core that determines jet mixing rather than the swirler vane angle. Consequently, the coaxial jet decays much faster, the mixing is more intense, and the turbulence intensities are higher for the  $35^\circ$  vane swirler. In view of these results, combustor designers should be more concerned with behavior of the solid-body rotation core produced by the swirler, instead of the swirler vane angle.

**Keywords:** swirling flows; variable-density mixing; combustor flows; confined turbulent flows; jet flows

## Introduction

Swirling flow is commonly used in gas turbine combustors to create a recirculation region for flame anchoring and to promote mixing between fuel and oxidant so that efficient burning can be accomplished in the shortest possible distance. Many different designs are used; some swirl the fuel jets, some swirl the secondary air jets, some swirl both jets in the same direction, while others swirl the jets in opposite directions. Although swirling is found to be most effective in accomplishing the design objectives of combustors, a systematic way of designing swirlers is not available. Consequently, swirler design for combustors has to be carried out on a trial-and-error basis. The reason for this is a lack of understanding of the fluid dynamics of confined swirling flow, especially concerning the mixing of different density fluids in a nonreacting as well as a reacting environment.

A comprehensive program of study to investigate the mixing of different density fluids in a nonreacting confined swirling flow, typical of those found in gas turbine combustors, had been initiated at Arizona State University several years ago. Since the phenomenon was very complex and there were numerous parameters of importance to the problem, the program, as a first attempt, identified several basic parameters for investigation:<sup>1-3</sup> (1) the swirl number, (2) the flow Reynolds number, (3) the jet-to-swirling-flow fluid density ratio, (4) the jet-to-swirling-flow velocity ratio, (5) the jet-to-swirling-flow momentum flux ratio, (6) the combustor geometry, and (7) the pressure drop behavior inside the combustor. In these investigations,<sup>1-3</sup> the combustor geometry was idealized by a swirler mounted in a cylindrical tube with a coaxial fuel jet. The Reynolds number effects were avoided by examining fully turbulent flows only. Also, the swirl imparted to the flow and created by a constant-angle vane swirler was fixed, and the resultant swirl number was 2.25. Pressure drop was found to have little effect on the resultant flow because its behavior was measured to be approximately linear, independent of jet fluid density and velocity. Therefore, these investigations reported on the effects

of parameters (3)–(5) at specified conditions for (1) and (6). The other parameters (2) and (7) were found to be not of primary importance. The results of these investigations showed that in the absence of a jet, a strong recirculation region was found in the tube core. It started at about one tube diameter downstream of the swirler and extended far downstream. When the jet fluid density was the same as the surrounding swirling flow, a jet with a very small momentum (0.07 of that of the swirling flow axial momentum) was found to be sufficient to destroy the recirculation region. Contrary to conventional wisdom, the swirling flow, instead of stabilizing the jet, promoted mixing of the jet with the surrounding fluid. This resulted in the complete disappearance of the jet at about two tube diameters downstream, independent of the jet momenta investigated. Consequently, the turbulence field in the combustor was found to be fairly isotropic. However, if the jet fluid density was less than that of the surrounding swirling flow, the recirculation region was found to be displaced from the tube core to a region away from the centerline. It was not destroyed. Instead, it served as a buffer to prevent mixing between the jet and the surrounding swirling fluid.<sup>2,3</sup> Consequently, the jet was preserved for a long distance inside the tube, and the resulting turbulence field was not as isotropic as the constant density flow. This difference in behavior between the two cases studied was directly attributed to the combined action of swirl and density difference between the jet and the surrounding flow.

Recognizing the importance of swirl on variable-density mixing in confined flows, the present investigation attempts to formalize the effects of swirl on such flows. In order to accomplish this objective, experiments similar to those reported in Refs. 1 and 2 were carried out with a different constant angle vane swirler. The swirler vane angle of the previous investigations was  $66^\circ$ , while the present investigation was conducted with a  $35^\circ$  vane swirler. As before, isothermal homogeneous (air into air) as well as inhomogeneous (helium into air) mixing was investigated. By comparing the present results with those in Refs. 1–3, the effects of swirl on variable-density mixing in confined flows can be assessed. Hopefully, this will lead to a

better understanding of the effects of swirl and swirler design on combustor flows.

## Brief review of previous work

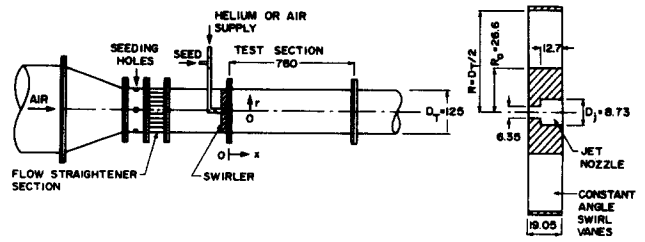
Swirl decay in pipe flows was examined by Yajnik and Subbaiah<sup>4</sup> and Weske and Sturov.<sup>5</sup> In the former study, small swirl was created by constant angle guide vanes, while in the latter, a solid-body rotation was produced in the flow by rotating the leading pipe at different speeds. In both cases, flow reversal was absent in the pipe. Swirl decay was found to be a strong function of the swirl number. However, even for the smallest swirl investigated, decay was not complete until 50 pipe diameters downstream of the swirler.

Swirl effects on the mixing of two streams with the same or different densities were investigated by a number of researchers.<sup>6-11</sup> Axisymmetric mixing layers were studied by Cheng<sup>6</sup> and Tan,<sup>7</sup> coaxial jet mixing was investigated by Vu and Gouldin,<sup>8</sup> while coaxial jets flowing into a sudden expansion was examined by Habib and Whitelaw,<sup>9</sup> Johnson *et al.*,<sup>10</sup> and Johnson and Roback.<sup>11</sup> The majority of these studies were on homogeneous mixing,<sup>6,8-11</sup> while Ref. 7 was on the mixing of two different density streams. The effects of swirling the external stream only were studied in Refs. 9-11, while the effects of swirling both streams in the same or opposite directions were examined in detail in Refs. 6-8. Finally, swirl effects on mixing in a reacting flow were examined by Brum and Samuelson.<sup>12,13</sup> They made measurements of the velocity field in an actual as well as a model combustor.

In all the above-mentioned studies, the researchers used a single swirler to create the swirling flow, and no attempt had been made to compare the effects of different swirlers on the resultant flow field produced in the combustor. Therefore, the present investigation represents a first attempt to compare the performance of different swirlers in the same combustor configuration; hopefully, this will lead to a better understanding of combustor designs.

## Experimental setup

The present experiments were carried out in the same facility as that used by So *et al.*<sup>1</sup> Briefly, it consisted of a vane swirler



NOTE: ALL DIMENSIONS IN mm

Figure 1 Test section schematic and swirler details

mounted concentrically into a Plexiglas tube of circular cross section. The tube had an inner diameter of 125 mm and a total length of 4.5 m, of which 0.76 m comprised the test section. A blower powered by a 25-hp variable-speed motor was used to deliver air to the tube through a contraction and a flow straightener section. Thus, the flow upstream of the swirler was uniform over 80% of the tube diameter and decreased rapidly inside the wall boundary layer to zero at the tube wall.<sup>14</sup> In this uniform central core region, a uniform turbulence level of  $\sim 5.5\%$  was also measured. A schematic of the test section is shown in Figure 1.

The swirler was of the vane design and has a jet nozzle arranged concentrically with the swirler (Figure 1). However, the constant-angle vanes do not extend all the way to the nozzle. A centerplate with a diameter of 53.18 mm separates the vanes from the nozzle. The nozzle was designed with a sudden expansion as shown in Figure 1. This design ensured that a turbulent jet would be produced by the nozzle even when the jet fluid was helium and the jet Reynolds number was 1500. The vane angle of this swirler was  $35^\circ$ . With the exception of the vane angle, the swirler used in the present study was identical to the one used in Refs. 1 and 2. In those studies the constant vane angle was  $66^\circ$ . The two swirlers produce a flow that is quite similar immediately downstream of the swirler; i.e., the flow is characterized by a constant flow angle equal to that of the vane angle and extending from the tube wall to the edge of the centerplane (see Figure 8). In view of this, the swirl number  $S$  across the vanes, defined as

$$S = \frac{\int_{R_0}^R U W r^2 dr}{R \int_{R_0}^R U^2 r dr} \quad (1)$$

### Notation

$c = W/r$	Slope of the solid-body rotation curve
$C$	Helium concentration
$D$	Diameter of tube or jet
$p$	Static pressure
$r$	Radial coordinate measured from tube centerline
$R$	Tube radius
$Re = \frac{U_{av} D_T}{\nu_a}$	Tube Reynolds number
$R_0$	Radius of centerplate in swirler
$S \approx \tan \theta$	Swirl number
$u$	Instantaneous axial velocity
$u'$	Rms $u$ velocity
$U$	Mean axial velocity
$\bar{U}$	Local average of $U$ across tube at any $x$ location
$U_{av} = \frac{1}{R^2} \int_0^R 2Ur dr$	Average of $U$ across tube at $x/D_T = -2$

$w$	Instantaneous circumferential velocity
$w'$	Rms $w$ velocity
$W$	Mean circumferential velocity
$x$	Axial coordinate measured from jet exit
$\theta$	Vane angle
$\nu$	Kinematic viscosity of fluid
$\rho$	Fluid density
$\psi = \tan^{-1} W/U$	Local flow angle

### Subscripts

$a$	Air or ambient condition
$h$	Helium
$j$	Jet
$o$	Centerline
$T$	Tube
$u$	Upstream of swirler at $x/D_T = -2$
$w$	Wall

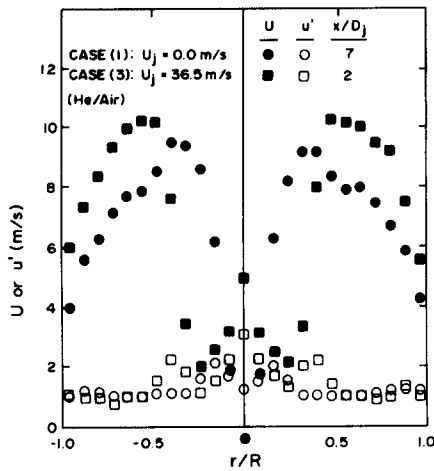


Figure 2 A check on flow symmetry

can be approximated by

$$S \cong \tan \theta \tag{2}$$

Therefore, the 35° and 66° vane swirlers can be characterized by  $S=0.7$  and 2.25, respectively.

Shop-compressed air and bottled helium were used as jet fluids. These were delivered to the jet nozzle via a heat exchanger to better control the jet fluid temperature. In all the experiments, the jet fluid temperature was conditioned to within 1°F of the air temperature in the tube. With this arrangement, true isothermal flow through the test section could be set up.

Velocity measurements were made with a DISA model 55L laser Doppler anemometer (LDA) equipped with a DISA 55N10 frequency shifter operating in the forward scatter mode. The coherent light source was provided by a 15-mw helium-neon laser (wavelength  $\lambda=632.8$  nm). All measurements of  $u$  were made in the horizontal plane passing through the tube axis; measurements of  $w$  were made in the vertical plane normal to the tube axis. The dimensions of the sampling volume were  $\sim 1$  mm long by 0.1 mm wide. Therefore, the uncertainty estimate for location was  $\sim 1.5\%$  of  $R$  in the measurement position due to finite length of sampling volume and possible nonuniformities in pipe wall thickness. As for velocity, the uncertainty estimate was  $\sim 2.5\%$  of  $U_{av}$  due to flow rate variations over time and possible nonuniformities in the size of the seeding particles.

Seeding the flow for laser measurements was accomplished by depositing droplets of glycerine-water solution, centered around 1  $\mu$ m in size, into the tube upstream of the swirler. Experiments had been carried out in Ref. 14 to determine the effects of seeding, if any, on the measured velocities when both the swirling flow and the jet were seeded compared to just seeding the swirling flow alone. No discernible differences in the measured  $U$  and  $W$  for air jet were observed at  $x/D=1$  and 40. For helium jets into air, repeatable measurements of  $U$  and  $W$  were possible only if the jet and the swirling flow were both seeded. As a result, experiments with pure helium jets were not possible, and a mixture of helium/air was used as jet fluid with the seeding droplets carried by an air stream introduced as shown in Figure 1. The helium concentration  $C_j$  and jet velocity  $U_j$  were measured at  $x/D_j=0.5$  with the test section removed and the co-flow turned off. A hot-wire-type concentration probe<sup>3</sup> was used to measure  $C_j$ , and LDA was used to measure  $U_j$ . For air jets, a pitot-static probe was also used to measure  $U_j$ , and the results were found to be in excellent agreement with the LDA-measured  $U_j$ . Since the concentration probe is not sensitive to the upstream velocity and has been

shown to be independent of fluid rotation,<sup>3</sup> its application to measure concentration in a swirling flowfield is quite valid. Even then, neither the concentration probe nor the pitot-static probe was used to measure  $C_j$  or  $U_j$  in the presence of a swirling flow. As a result, these measurements were not influenced by swirl at all.

### Test conditions

All the experiments of Refs. 1 and 2 were carried out at a fixed swirler upstream flow condition. This was characterized by  $U_{av}=6.8$  m/s and a Reynolds number,  $Re$ , of  $5.49 \times 10^4$ . The same upstream flow condition was maintained for the present experiments. Altogether, three sets of experiments were carried out: (1)  $U_j=0$ , (2) air jet with  $U_j=25.4$  m/s, and (3) helium/air jet with  $U_j=36.5$  m/s. The density ratios,  $\rho_j/\rho_a$ , for (2) and (3) are 1 and 0.228, respectively, and the corresponding  $Re_j=U_j D_j/\nu_j$  are 14,380 and 2970, respectively. These test conditions were identical to some of the cases studied in Refs. 1 and 2 and allowed the present results to be compared for possible swirl effects on confined jet mixing with and without density difference.

Flow symmetry in the test section was checked by measuring  $U$  and  $u'$  across the tube at three different  $x/D_j$  locations between  $1 \leq x/D_j \leq 40$ . For the three cases (1)–(3) examined, both  $U$  and  $u'$  were found to be quite symmetric about the tube axis. A sample plot of these measurements is shown in Figure 2. Consequently, all subsequent measurements were carried out across the tube radius only.

The axial wall pressure  $p_w$  along the test section was also measured to see if the jet and density difference have any effect on the resultant  $p_w$  distribution. A plot of  $(p_u - p_w)/(1/2)\rho_a U_o^2$  versus  $x/D_j$  is shown in Figure 3. Here,  $U_o$  at  $x/D_j=-2$  is used to evaluate the dynamic pressure. The pressure drop curves for cases (1)–(3) are shown together with the corresponding measurements from Refs. 1 and 2. It can be seen that the pressure drop behavior is the same for cases (1)–(3) and for both swirlers, even though the pressure drop level is different for the two swirlers. In view of this, the axial pressure drop behavior is not affected by the presence of a central jet with or without density difference. Therefore, this allows the present results to be compared with those of Refs. 1 and 2 and the effects of swirl on different density jet mixing to be analyzed.

### Presentation of results

Due to variations in blower capacity over time,  $U_{av}$  is found to vary by as much as 8% over the duration of these experiments. However, the variations over any one run are far less and are

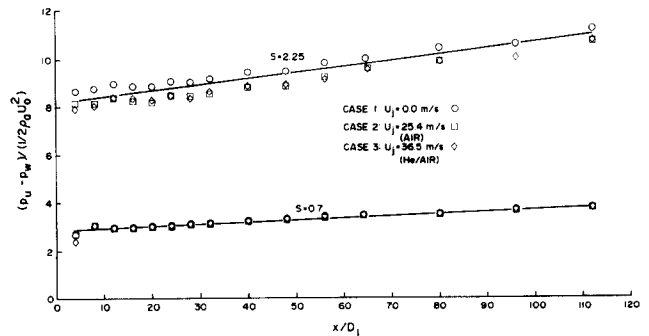


Figure 3 Pressure drop along test section

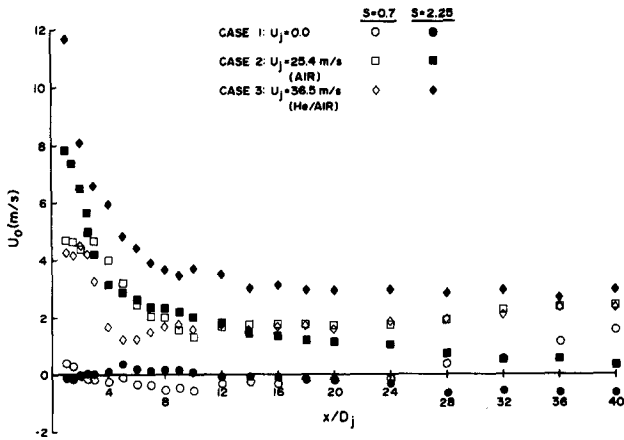


Figure 4 Comparison of centerline decay of  $U_0$  for the two swirlers

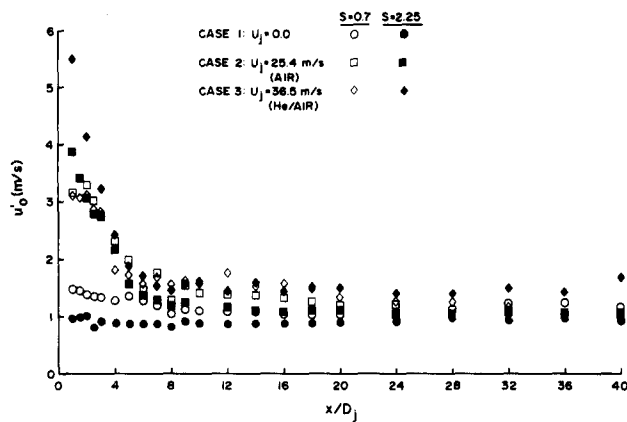


Figure 5 Comparison of centerline decay of  $u'_0$  for the two swirlers

about 2%. Therefore, this suggests that all velocity results should be presented by normalizing with the local  $\bar{U}$  rather than  $U_{av}$ . In order to determine  $\bar{U}$  in the absence of helium concentration measurements, the following approximation is made. Since the mass flux through the tube in the absence of the jet is  $\sim 103$  g/m/s and the mass fluxes added to the tube due to the air and helium/air jets are 1.8 g/m/s and 0.5 g/m/s, respectively, the added mass flux to the swirling flow is small and is masked by fluctuations in the swirling-flow mass flux caused by variations in blower capacity. This is especially true for case (3), where the added mass flux is only 0.5 g/m/s compared with a mass flux of  $\sim 103 \pm 2$  g/m/s in the swirling flow. In view of this,  $\bar{U}$  at any  $x$  locations downstream of the swirler can be approximated by

$$R^2 \bar{U} = \int_0^R 2Ur \, dr \quad (3)$$

This definition of  $\bar{U}$  is exact for case (2), but would give a small error for case (3). However, this small error is negligible compared to variations in blower capacity that resulted in a 2% variation in the swirling-flow mass flux measurements.

Velocity measurements at 10 different  $x$  locations spanning the range  $1 \leq x/D_j \leq 40$  for cases (1)–(3) are available. In addition, centerline measurements of  $U_0$ ,  $u'_0$ , and  $w'_0$  are carried out at 22 locations between  $1 \leq x/D_j \leq 40$ . All these results for the  $35^\circ$  swirler ( $S=0.7$ ) are presented in Ref. 15. Similarly, detailed measurements are reported in Refs. 1 and 2 for the  $66^\circ$  swirler ( $S=2.25$ ). In the following comparison, selected velocity

measurements at a few locations are shown to illustrate the difference in the resultant flow field created by the two swirlers. A comparison of centerline decay of  $U_0$ ,  $u'_0$ , and  $w'_0$  for cases (1)–(3) between the two swirlers ( $S=0.7$  and  $2.25$ ) is shown in Figures 4–6. The detailed characteristics of the swirling flow alone (case 1) are analyzed in Figures 7–10, while a comparison of the effects of swirl on homogeneous (case 2) and inhomogeneous (case 3) jet mixing in a confined flow is presented in Figures 11–14.

The centerline measurements of  $U_0$  (Figure 4) show that the  $S=0.7$  swirler gives rise to one recirculation region extending from  $x/D_j=2$  to  $x/D_j=26$ . On the other hand, the  $S=2.25$  swirler gives rise to two recirculation regions: one in the region  $0 \leq x/D_j \leq 3$ , and another extending from  $x/D_j=15$  to beyond  $x/D_j=40$ . Since the two swirlers are of the same design and the only difference is in the vane angle, this difference in behavior along the tube centerline is a direct consequence of the radial pressure gradient set up by the swirlers. This result also tends to indicate that swirl in the flow decays much faster for the  $S=0.7$  swirler than for the  $S=2.25$  swirler. Further evidence in support of this interpretation can be gleaned from the plots of  $W$  and  $\psi$  shown in Figures 7 and 8. In Figure 8, the local flow angle at three different  $x/D_j$  locations for the two swirlers are compared. The actual  $W$  distributions across the tube at the same  $x/D_j$  locations are shown in Figure 7. A rapid decay of the flow angle  $\psi$  in the tube core for the  $S=0.7$  swirler is clearly evident. Even though both swirlers set up a solid-body rotation of the fluid in the tube core, the slope of the curve,  $c=W/r$ , is different (Figure 7). At  $x/D_j=1$ ,  $c \approx 1600 \text{ s}^{-1}$  for the  $S=0.7$  swirler and  $c \approx 811 \text{ s}^{-1}$  for the  $S=2.25$  swirler. However, at  $x/D_j=40$ ,  $c$  decreases to  $\sim 1080 \text{ s}^{-1}$  and  $\sim 700 \text{ s}^{-1}$ , respectively, for the  $S=0.7$  and  $2.25$  swirlers. This means that fluid rotation is much faster near the tube core and the decay of swirl is much more rapid for the  $S=0.7$  swirler. Furthermore, the extent of the solid-body rotation core for the  $S=0.7$  swirler is only about one third of that for the  $S=2.25$  swirler. The effect of this difference in behavior on jet mixing will be analyzed later.

The flow characteristics produced by the two swirlers not only differ in the  $W$  distributions, but also show substantial difference in the  $U$  distributions (Figure 9). For the  $S=2.25$  swirler, the  $U$  velocity at  $x/D_j=1$  drops to  $\sim 0$  at the edge of the centerplane and remains constant from this point on to the tube center. On the other hand, the  $U$  velocity profile at  $x/D_j=1$  produced by the  $S=0.7$  swirler shows a maximum at the edge of the centerplane and another maximum at the edge of the nozzle. Essentially, the same differences persist between

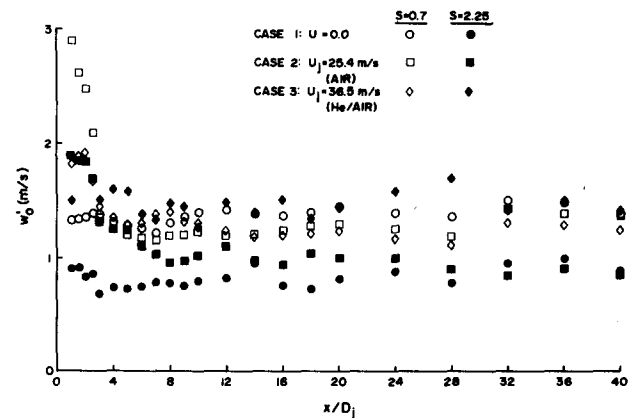


Figure 6 Comparison of centerline decay of  $w'_0$  for the two swirlers

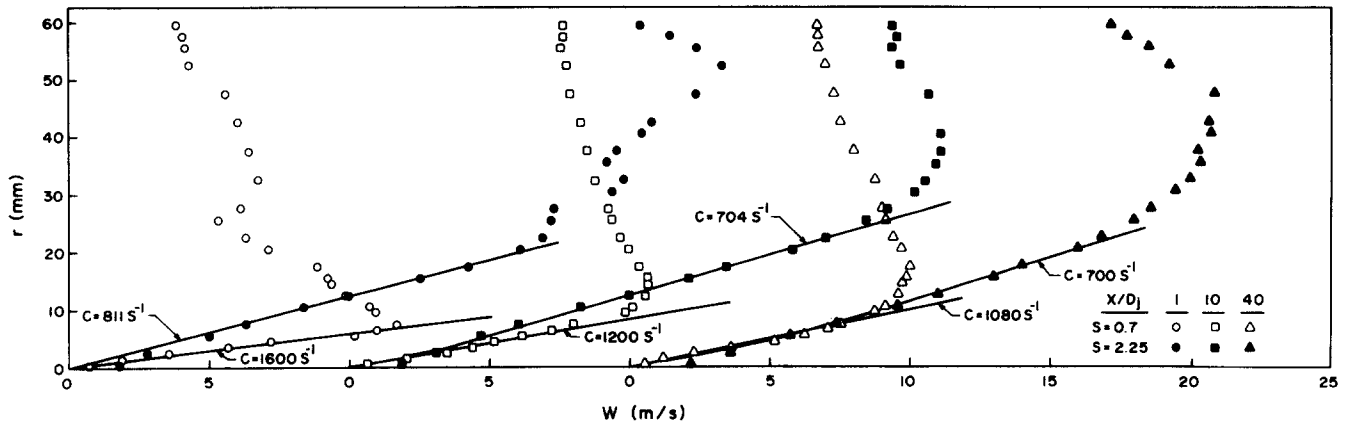


Figure 7 Characteristics of the solid-body rotation core

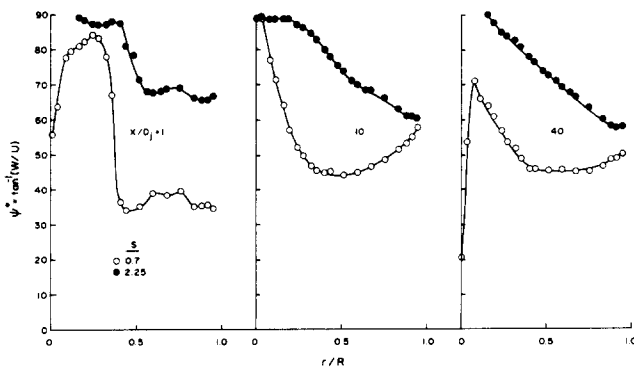


Figure 8 A comparison of local flow angle ( $\psi$ ) for the two swirlers

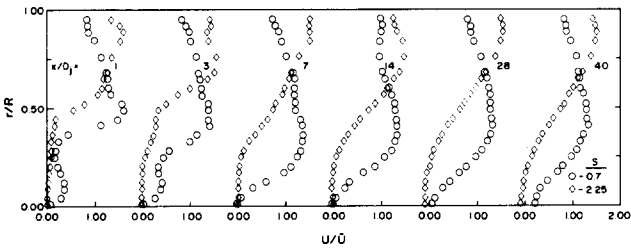


Figure 9 Behavior of  $U$  for the two swirlers

the  $U$  distributions created by the two swirlers as the flow moves downstream. The turbulence fields produced by the two swirlers also show the same kind of differences (Figure 10), and these are still evident even at  $x/D_j = 40$ . One important point to note is that  $u' \approx w'$  at  $x/D_j = 40$  for the  $S = 2.25$  swirler, but is quite different for the  $S = 0.7$  swirler, especially near the tube core. Whether these differences will also have an effect on jet mixing will be analyzed later.

Even though the centerline  $u'_0$  for the  $S = 0.7$  swirler is initially higher than that for the  $S = 2.25$  swirler, it decays to the same level at about  $x/D_j = 20$  (Figure 5). However, the difference in  $w'_0$  produced by the two swirlers persists throughout the region investigated (Figure 6). This is purely a consequence of the difference in flow characteristics created by the swirlers. Although the two swirlers are of the same design with only the vane angle different, the resultant flow fields created by the two swirlers differ greatly in character.

Jets in a co-flowing stream had been investigated by a number of researchers.<sup>16-19</sup> These included both experimental work on

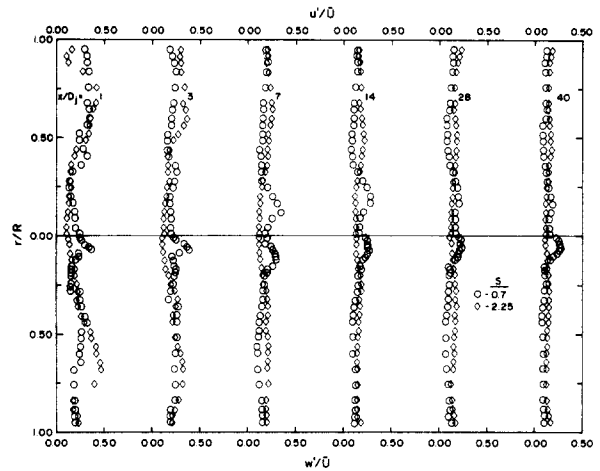


Figure 10 Behavior of  $u'$  and  $w'$  for the two swirlers

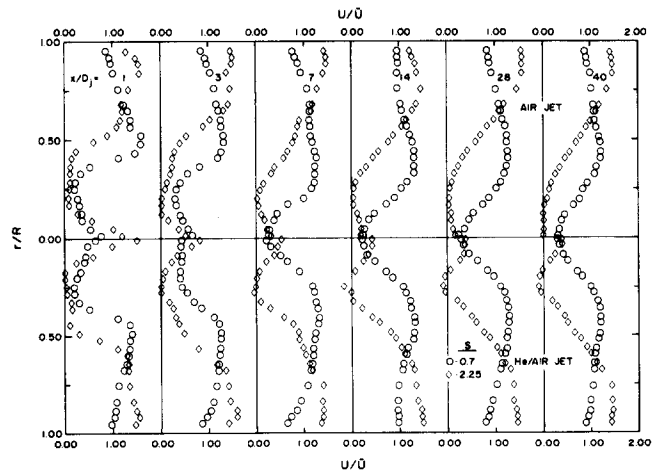


Figure 11 Behavior of  $U$  with a central jet for the two swirlers

isothermal<sup>16,17</sup> and nonisothermal<sup>18</sup> mixing and semianalytical work on the prediction of jet decay.<sup>19</sup> In all these studies the jet was found to decay a lot faster than free jets, and a potential core was not observed even for an external-stream-to-jet velocity ratio of 0.1. Furthermore, the centerline distribution of  $u'_0$  was found to increase as the external-stream-to-jet velocity increases. These results were essentially a consequence of the increased mixing between the jet and the external stream. Since

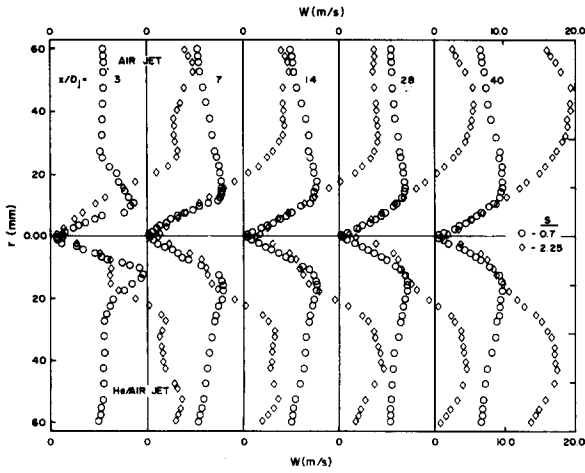


Figure 12 Behavior of  $W$  with a central jet for the two swirlers

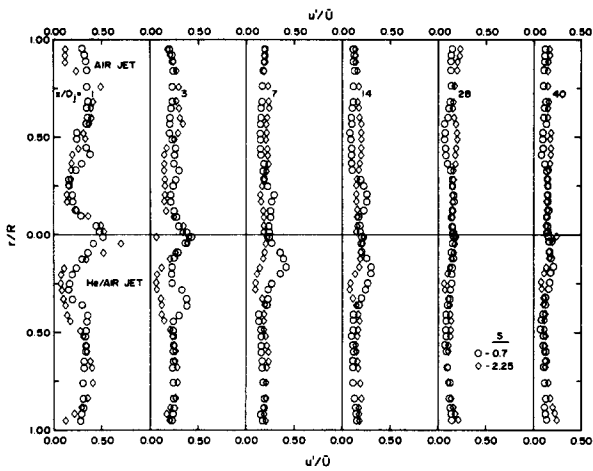


Figure 13 Behavior of  $u'$  with a central jet for the two swirlers

swirl tends to promote mixing, one could conjecture that the jet would decay even faster when the external stream is swirling. This conjecture is partly substantiated by the measurements of Refs. 1 and 2. Furthermore, one would expect the degree of swirl to have a marked effect on the jet decay; i.e., as  $S$  increases, the decay of the jet would become faster. On the other hand, the present results ( $S=0.7$ ) show that the jets actually decay faster than the high swirl ( $S=2.25$ ) cases (Figure 4). The reason for this behavior can again be found in the characteristics of the solid-body rotation core. Since the centrifugal acceleration experienced by a fluid element in a swirling flow is  $r(W/r)^2$ , the centrifugal force acting on the element will be larger for larger values of  $c = W/r$ . Therefore, jet mixing is dependent on  $c$  rather than on  $S$ . The  $S=0.7$  swirler gives a solid-body rotation core with a  $c$  about twice that for the  $S=2.25$  swirler. Consequently, the jets in this case decay faster than in the high swirl case.

The mass flux through the tube in the absence of the jet is  $\sim 103$  g/m/s. For cases (2) and (3), the mass fluxes added to the tube due to the air and helium/air jets are 1.8 g/m/s and 0.5 g/m/s, respectively. In terms of total jet to total axial momentum flux ratio, the values are 0.068 and 0.032, respectively. Therefore, the added mass and momentum fluxes to the swirling flow are small. However, their effects on the swirling flow, especially near the tube core, are quite large. A concentrated air jet of small momentum is sufficient to eliminate the reversed flow regions in the tube core (Figure 11) in the region investigated. When the jet fluid is helium/air mixture ( $\rho_j/\rho_a =$

0.228), the effect on the swirling flow is different for the two swirlers. For the  $S=0.7$  swirler, the reversed flow region is completely erased, while for the  $S=2.25$  swirler, the first reversed flow region is destroyed by the jet, but the second reversed flow region is displaced outward toward the tube wall (Figure 11). As a result, the helium/air jet is preserved and is still noticeable at  $x/D_j=40$ . Ahmed *et al.*<sup>2</sup> attribute this behavior to the combined effects of swirl and density difference. The lighter helium element which carries with it a smaller centrifugal force is being pushed back to the tube center by the larger radial pressure gradient set up by the swirling motion. On the other hand, the initial large decay of the helium/air jet caused by the  $S=0.7$  swirler resulted in a thorough mixing of the helium element with the surrounding air and this leads to a complete disappearance of the helium/air jet. Furthermore, the reversed flow region created by the  $S=0.7$  swirler begins at  $x/D_j=2$ , which is quite a bit closer to the jet exit, compared with the second reversed flow region created by the  $S=2.25$  swirler, which begins at  $x/D_j=15$ . Therefore, the added axial momentum is more effective in destroying the reversed flow region for the  $S=0.7$  swirler. This result indicates that it is not the swirler vane angle that controls jet mixing in confined swirling flow when the jet fluid is lighter than the surrounding swirling fluid. Rather, it is the solid-body rotation core created by the swirler. In view of this, combustor designers should pay more attention to the swirling flow behavior near the core instead of the overall swirl behavior commonly characterized by the vane angle or swirl number.

Introduction of an air jet into the confined swirling flow does not affect the behavior of the solid-body rotation core when the added jet momentum is small (Figure 12). Essentially, the same slopes ( $c$ ) as those shown in Figure 7 are measured for both swirlers at  $x/D_j=1$  and 40 for case (2), and the  $W$  distributions beyond the solid-body rotation core are also not affected by the presence of the jet. When the jet fluid is lighter than the swirling air, the resultant  $W$  distributions depend to a large extent on the swirler. For the  $S=0.7$  swirler, the reversed flow region in the tube core is destroyed by the helium/air jet, and the resultant  $W$  distributions are unaffected (Figure 12), just as in case (2). However, for the  $S=2.25$  swirler, the second reversed flow region in the tube core is displaced outward toward the wall by the helium/air jet, and the resultant  $W$  distributions are modified by the movement of this reversed flow region. A plateau in the  $W$  distributions is noticed in the region  $0.12 < r/R < 0.25$  (Figure 12), which coincides with the region occupied by the reversed flow (Figure 11). According to Ahmed and So,<sup>3</sup>

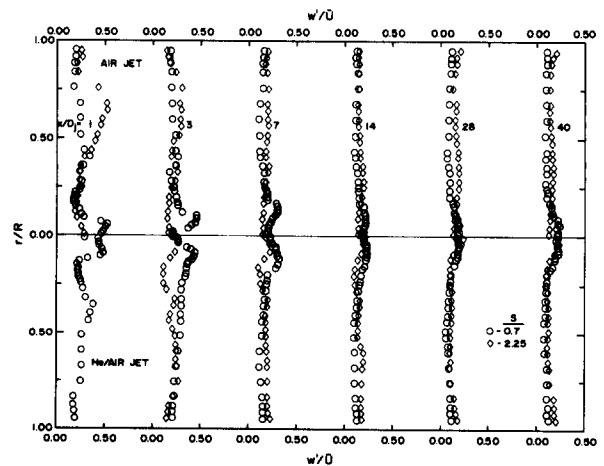


Figure 14 Behavior of  $w'$  with a central jet for the two swirlers

this reversed flow region serves as a buffer between the external swirling air and the central helium/air jet. It is in this region that the helium concentration decreases to zero from its maximum at the jet centerline. Since the reversed flow velocity is very small in this region, the whole region tends to rotate around with a constant  $W$ . This behavior remains distinct even at  $x/D_j = 40$ . In view of this, the  $S = 2.25$  swirler does not perform as well as the  $S = 0.7$  swirler in terms of promoting mixing between the helium/air jet and the external swirling air.

The jet only affects the turbulence field along the tube core (Figures 13 and 14). Beyond this region, the  $u'$  and  $w'$  distributions are essentially the same as those measured in the absence of the jet. Furthermore, their behavior is the same for air as well as helium/air jets (compare Figure 10 with Figures 13 and 14). This shows that the turbulence field in the tube outside of the jet region is independent of the jet when the added jet momentum is small.

## Conclusions

Three main conclusions emerge from this study. First, the flow produced by two swirlers of the same design but with different vane angles is totally different. The major difference appears in  $W$ . Even though the vane angle of one swirler is about half that of the other, the slope of the solid-body rotation core is about twice as large. It is this local behavior that determines jet mixing and decay rather than the overall swirl number of the flow. Second, the  $S = 0.7$  swirler performs better in terms of promoting mixing between a lighter central jet and the external swirling air, compared with the  $S = 2.25$  swirler. In the latter case, the helium/air jet is confined along the tube core by a reversed flow region which serves as a buffer between the swirling air and the helium. Finally, jet decay is governed by the characteristics of the solid-body rotation core. A tighter solid-body rotation core offers more resistance to the incoming jet and thus causes it to spread more rapidly radially and eventually leads to faster decay of the jet. In view of this finding, combustor designers should pay more attention to the characteristics of the solid-body rotation core produced by the swirler instead of the overall characteristics of the swirling flow.

## Acknowledgment

Research support by NASA Grant NAG3-260, monitored by Dr. J. D. Holdeman, is gratefully acknowledged.

## References

- 1 So, R. M. C., Ahmed, S. A. and Mongia, H. C. Jet characteristics in confined swirling flow. *Exp. Fluids*, 1985, 3, 221–230
- 2 Ahmed, S. A., So, R. M. C. and Mongia, H. C. Density effects on jet characteristics in confined swirling flow. *Exp. Fluids*, 1985, 3, 231–238
- 3 Ahmed, S. A. and So, R. M. C. Concentration distributions in a model combustor. *Exp. Fluids*, 1986, 4, 107–113
- 4 Yajnik, K. S. and Subbaiah, M. V. Experiments on swirling turbulent flows. Part 1: Similarity in swirling flows. *J. Fluid Mech.*, 1973, 60, 665–687
- 5 Weske, D. R. and Sturov, G. Yu. Experimental study of turbulent swirled flows in a cylindrical tube. *Fluid Mech.—Soviet Res.*, 1974, 3, 77–82
- 6 Cheng, W. K. Turbulent Mixing in Swirling Flow. MIT GT and PDL Rept. 143, 1978
- 7 Tan, C. S. An Experimental Study of the Effects of Swirl and Density Difference on Mixing in Shear Flows. MIT GT and PDL Rept. 153, 1980
- 8 Vu, B. T. and Gouldin, F. C. Flow measurements in a model combustor. *AIAA J.*, 1982, 20, 642–61
- 9 Habib, M. S. and Whitelaw, J. H. Velocity characteristics of confined coaxial jets with and without swirl. *J. Fluids Eng.*, 1980, 102, 47–53
- 10 Johnson, B. V., Roback, R. and Bennett, J. C. *Scalar and Momentum Turbulent Transport Experiments with Swirling and Nonswirling Flows*. ASME, Special Publication AMD-66, eds. R. M. C. So, J. H. Whitelaw, and M. Lapp, 1984, 107–119
- 11 Johnson, B. V. and Roback, R. Mass and momentum turbulent transport experiments with confined swirling jets. AIAA Paper No. 84-1380, 1984
- 12 Brum, R. D. and Samuelson, G. S. Assessment of a dilute swirl combustor as a bench scale, complex flow test bed for modeling diagnostics, and fuels effects studies. AIAA Paper No. 82-1263, 1982
- 13 Brum, R. D. and Samuelson, G. S. *Two-Component Laser Anemometry Measurements of Non-Reacting and Reacting Complex Flows in a Swirl-Stabilized Model Combustor*. ASME, Special Publication AMD-66, eds. R. M. C. So, J. H. Whitelaw, and M. Lapp, 1984, 275–290
- 14 So, R. M. C., Ahmed, S. A. and Mongia, H. C. An experimental investigation of gas jets in confined swirling air flow, NASA CR-3882, 1984
- 15 Majidi, R. Effects of swirl on confined jet mixing. MS Thesis, Arizona State University, MAE Dept., 1985
- 16 Antonia, R. A. and Bilger, R. W. An experimental investigation of an axisymmetric jet in a co-flowing air stream. *J. Fluid Mech.*, 1973, 61, 805–822
- 17 Biringen, S. An experimental investigation of a turbulent round jet in a co-flowing airstream. ASME Paper No. 86-WA/FE-13, 1986
- 18 Antonia, R. A. and Bilger, R. W. The heated round jet in a co-flowing stream. *AIAA J.*, 1976, 14, 1541–1547
- 19 Antonia, R. A. and Bilger, R. W. The prediction of the axisymmetric turbulent jet issuing into a co-flowing stream. *Aero. Quarter.*, 1974, 25, 69–80